I.Yu. Yermolenko, M.V. Ved', A.V. Karakurkchi, N.D. Sakhnenko, Z.I. Kolupayeva

THE ELECTROCHEMICAL BEHAVIOR OF Fe^{3+}–WO_4^{2-}–Cit^{3-} AND Fe^{3+}–MoO_4^{2-}–WO_4^{2-}–Cit^{3} SYSTEMS

National Technical University "Kharkiv Polytechnic Institute", Kharkiv, Ukraine

The kinetic parameters of electrochemical behavior of tungsten at the deposition of Fe–W and Fe–Mo–W alloys were determined using linear voltammetry and analyzing polarization relationships. In the presence of citrate ions the cathode process was shown to proceed with the participation of $[FeHCitWO_4]^-$ clusters. An optimal concentration ratio of the components in electrolyte required for the Fe–W alloy deposition was defined as $c(Fe^{3+}):c(Cit^{3-}):c(WO_4^{2-}) = 1:1.5:0.3$. The deviation from this ratio by an increase in the concentration of tungstate ions results in the formation of dimer forms $W_2O_7^{2-}$ and $[FeW_2O_7HCit]^-$ clusters; as a result the concentration of electrode active particles $[FeWO_4HCit]^-$ diminishes and the cathode process is inhibited. A peculiar feature of the formation of electrolytic alloy Fe–Mo–W is a competitive reduction of molybdates and tungstates. Based on the analysis of the kinetic parameters and characteristic criteria of electrochemical reactions, we proposed the mechanism for the co-deposition of alloy containing iron with molybdenum and tungsten; this mechanism is a sequence of coupled reactions of irreversible reduction of intermediates with slow charge transfer stage and previous chemical step of the ligands release. The data of X-ray phase analysis show that the binary alloys Fe–W are solid solutions of tungsten in iron and ternary alloys Fe-Mo-W are X-ray amorphous.

Keywords: tungsten, alloys, iron, kinetics, citrate electrolyte, electrodeposition.

Introduction

The scientists and technologists pay a great attention to binary and ternary metal alloys of iron triad with refractory components, in particular molybdenum and tungsten, trying to get the materials whose functional properties and service performances considerably supersede those of alloy-forming components [1,2].

The problem of prediction of the composition and properties still remains to be a main barrier on the way to the broad introduction of the process of electrochemical synthesis of binary and ternary alloys of the iron family with d^4-elements. This is related to relatively complicated and ambiguous processes that occur in the electrolyte and at the inter-phase boundary at the cathode polarization.

Many scientific papers are devoted to the synthesis of binary alloys Fe(Ni, Co)–Mo(W) using the electrolytes of a different qualitative and quantitative composition, however scientific circles have no common conception of the mechanism of co-precipitation of given metals into the alloy.

The authors believe [3] that the most probable mechanism for the co-deposition of cobalt with molybdenum from the citrate electrolyte is the reduction of oxo-anion to get the intermediate oxide MoO_2 in the presence of citrate cobalt clusters that act in this case as a catalyst:

$$MoO_4^{2-} + 2H_2O + 2\bar{e} \xrightarrow{CoCit^-} MoO_2 + 4OH^-, \quad (1)$$

with further formation of the adsorbed intermediate following the mechanism offered in [4]:

$$CoCit^- + 2\bar{e} \rightarrow Co + Cit^{3-}; \quad (2)$$

$$CoCit^- + MoO_2 \rightarrow [MoO_2 - CoCit^-]_{ad}; \quad (3)$$

$$[MoO_2 - CoCit^-]_{ad} + 2H_2O + 4\bar{e} \rightarrow \rightarrow Mo + CoCit^- + 4OH^-. \quad (4)$$

Younes et al. [5] supposed that the electrode-active mixed citrate cluster of nickel and tungsten is formed in the solution or on the electrode surface, which is the precursor for the nickel and tungsten alloy synthesis. However they failed to prove the presence of these particles in the solution. Nevertheless, the paper [6] demonstrated an indirect evidence of the mixed nickel-tungstate-citrate cluster formation in the reaction:

$$[(Ni)(Cit)]^- + [(WO_4)(Cit)(H)]^{4-} \rightarrow \rightarrow [(Ni)(WO_4)(Cit)(H)]^{2-} + Cit^{3-}. \quad (5)$$

The data of gel-chromatographic division of citrate [7] and gluconate [8] electrolytes into the components with different molecular masses also support the hypothesis on the formation of mixed clusters. This allows us to arrive at a conclusion that citrate and multinuclear hetero-metal clusters are formed that are the precursors for the deposition of cobalt-tungsten alloys.

Special attention is paid to the process of electrolytic iron alloys deposition, for example, Fe-Mo(W) and Fe–Mo–W, that has a distinction in kind, in particular it has an opportunity to use the electrolytes both on the basis of iron(II) and iron(III) [9]. It should be noted that the tendency of iron to the hydrolysis has a substantial influence of the pH electrolyte on the ion equilibrium in the water solution, and consequently on the nature of electrode-active particles [10,11].

Due to the above reasons and in spite of the fact that the control deposition process of the coatings by multicomponent alloys of a given composition is based on general regulations of electroplating technique, it is empirical in many respects and requires the improvement of many methodological aspects. To achieve the set goal and correct interpretation of electrochemical behavior of the Fe^{3+}–Cit^{3-}–MoO_4^{2-}–WO_4^{2-}–H_2O system it is necessary to analyze the kinetic of cathode processes in Fe^{3+}–Cit^{3-}–MoO_4^{2-}–H_2O and Fe^{3+}–Cit^{3-}–WO_4^{2-}–H_2O systems as basic mechanisms for the deposition of Fe–W and Fe–Mo–W alloys.

Experimental

The kinetics of cathode processes was studied using the electrodes made of low-carbon steel (Steel 3) with the working area of $7.8 \cdot 10^{-2}$ cm^2 in the solutions with a constant concentration of iron(III) sulfate and sodium citrate and the concentration of sodium molybdate and sodium tungstate varying in the range of 0.004 to 0.008 mol/dm^3 in 1 M Na_2SO_4 solution as supporting electrolyte (Table 1). The electrolyte solutions were prepared using the certified reagents of chemically pure grade on the distilled water. The acidity of working solutions was controlled by pH-meter pH-150M with the glass electrode ESL-6307.

Voltammetric measurements were taken in the three-electrode glass cell with the chloride-silver reference electrode EV-1M1 and auxiliary platinum electrode. The paper gives all the potentials with regard to standard hydrogen electrode (SHE). The polarization was conducted using the potentiostat PI-50-1.1 with the programmer PR-8; the potential scanning rate varied in the range of $2 \cdot 10^{-3}$–$1 \cdot 10^{-1}$ V/s. Output parameters were registered by the computer using special-purpose "Polarization" software.

Table 1

The composition of electrolytes used for kinetic investigation

Component	Concentration, mol/dm^3		
	Fe–Mo	Fe–W	Fe–Mo–W
Na_2SO_4	1	1	1
Fe^{3+}	0.02	0.02	0.02
Cit^{3-}	0.03	0.03	0.03
MoO_4^{2-}	0.005–0.008	–	0.006
WO_4^{2-}	–	0.004–0.008	0.004–0.008

To analyze the experimental data and define kinetic regularities and the mechanism of cathode reactions, we used the following kinetic parameters and characteristic criteria [12]: the peak potential E_p and semi-peak potential $E_{p/2}$ (V); the peak current density i_p (A/dm^2); the product of the transfer coefficient and the electron number αz; the orders of reactions p_i, the Semerano criterion X_s and the concentration criterion X_c.

To verify the data, the αz product for the irreversible step (stage) was defined using two modes:

– an angle coefficient of the relationship in E_p–lgs coordinates:

$$\frac{\Delta E_p}{\Delta \lg s} = -\frac{2,303RT}{\alpha zF}; \quad (6)$$

– Matsuda and Ayabe equation:

$$E_p - E_{p/2} = -1.85\frac{RT}{\alpha zF}, \quad (7)$$

where s is the sweep rate (V/s), R is the universal gas constant, and T is the thermodynamic temperature (K).

Apparent orders of the reaction, p_i, were calculated using the concentration relationships of the rate of irreversible electrode reaction as a function of components at a constant content of other components:

$$p_i = \frac{\Delta \lg i_E}{\Delta \lg c_i}, \quad (8)$$

where i_E is the current density for the prescribed potential, c_i is the concentration of the i-th kind of ions in the solution.

The chemical composition and morphology of coatings were defined using the X-ray fluorescent method and portable spectrometer "SPRUT" with a relative standard error of 10^{-3}–10^{-2}, the measurement error of the percentage of components was equal to ±1 wt.%. To verify the data, the energy-dispersive X-ray spectroscopy was performed using

the electron-probe microanalyzer Oxford INCA Energy 350 integrated into the SEM system. The X-ray radiation was induced by the exposure of specimens to the electron beam of 15 keV. The patterns were obtained by the registration of secondary electrons (BSE) with the electron beam scanning, which allowed us to study the topography with a high resolution and contrast.

The phase composition of coatings was studied using the method of X-ray analysis. The survey was done using the X-ray diffractometer DRON-2.0 in the iron anode radiation. The diffraction pattern was recorded in the discrete mode every other 0.1° with the exposition at each point of 20 s. To define the phase composition the specimens Fe–W and Fe–Mo–W on the mild steel were used with the alloy coating thickness h of at least 20 mm.

Theoretical aspects

A physical and chemical purport of the "induced co-deposition" of iron with molybdenum and tungsten mentioned frequently enough in the scientific papers written by home and foreign authors [4] consists in coupled and interdependent electro-reduction of two and more metals, because molybdenum and tungsten are not reduced individually out of water solutions to acquire the metal state.

Similar values of the equilibrium potentials of electrode reactions for the step reduction of iron(III) and molybdates serve as the prerequisites for the formation of electrolytic alloy Fe–Mo:

$$Fe^{3+}+\bar{e}=Fe^{2+},$$
$$E_e=0.77+0.059\lg[c(Fe^{3+})/c(Fe^{2+})]; \quad (9)$$

$$Fe^{2+}+2\bar{e}=Fe^{0},$$
$$E_e=-0.44+0,0295\lg c(Fe^{2+}); \quad (10)$$

$$MoO_4^{2-}+4H^{+}+2\bar{e}=MoO_2+2H_2O,$$
$$E_e=0.606-0.1182pH+0.0295\lg c(MoO_4^{2-}); \quad (11)$$

$$MoO_4^{2-}+8H^{+}+3\bar{e}=Mo^{3+}+4H_2O,$$
$$E_e=0.508-0,1576pH+$$
$$+0.0197\lg[c(MoO_4^{2-})/c(Mo^{3+})]; \quad (12)$$

$$MoO_2+4H^{+}+4\bar{e}=Mo+2H_2O,$$
$$E_e=-0.072-0.059pH. \quad (13)$$

A similar situation is peculiar to the deposition of Fe–W alloys for the joint step reduction of iron(III) and tungstates:

$$WO_4^{2-}+4H^{+}+2\bar{e}=WO_2+2H_2O,$$
$$E^0=0.386-0.1182pH+0.2951\lg c(WO_4^{2-}); \quad (14)$$

$$WO_2+4H^{+}+4\bar{e}=W+2H_2O,$$
$$E^0=-0.119-0.0591pH. \quad (15)$$

The analysis of given relations shows that an assumption of the competitive reduction of molybdates and tungstates for the Fe–Mo–W coating deposition seems to be quite substantiated. Standard potentials of the reactions (14), (15) are lower in comparison with the participation of molybdates, therefore the probability of the progress of these reactions with the same concentration of oxo-anions is lower.

The availability of identical volume-centered cubic crystal lattices will contribute to the energetically easier joint crystallization. However, on the other part the difference in the lattice parameters will undoubtedly result in its distortion and deceleration of the linear growth of crystals and in this case we can expect the formation of somatoid (spheroid) structures. It should also be taken into account that the atomic radius of molybdenum and tungsten exceed the atomic radius of iron by 11 and 20%, accordingly (Table 2), therefore during the formation of mono-atomic layer the attached atoms are forced to dislocate from equilibrium positions, increasing thus a probability of the realization of "polycrystalline to amorphous" transition with regard to the state of the films of deposited alloys [13].

Table 2

Crystal-chemical parameters of alloying components

Parameters	Elements		
	Fe	Mo	W
Atomic radius, nm	0.117	0.130	0.141
The ionization energy, eV	7.87	7.10	7.98
Lattice structure	bcc lattice	bcc lattice	bcc lattice
Lattice parameters, E	2.866	3.147	3.160

Similar values of the first ionization potentials of iron and tungsten are a prerequisite for the formation of covalent bonds between the atoms and therefore a possibility of the co-deposition of tungsten and iron into the alloy with the formation of inter-metallides should not be excluded.

Results and Discussion

The Fe^{3+}–Cit^{3-}–MoO_4^{2-}–H_2O, Fe^{3+}–Cit^{3-}–WO_4^{2-}–H_2O and Fe^{3+}–Cit^{3-}–MoO_4^{2-}–WO_4^{2-}–H_2O systems are extremely complicated and mobile from the standpoint of ion equilibriums and it is impossible to mark out the partial relationships of the reduction of molybdenum and tungsten, because these cannot be reduced independently in the form of individual metals out of water solutions. Therefore, from our point of view it is correct to speak about the formal kinetics with regard to the processes with the participation of molybdenum and tungsten.

It was shown earlier [14] that the pH of electrolyte from which the Fe–Mo alloy is deposited remains to be constant in the range of studied molybdate-ion concentrations and it is equal to 3.3.

The cathode process with the participation of $[FeHCit]^+$ and $[FeHCitMoO_4]^-$ clusters is multistage and proceeds through the formation of molybdenum oxides of a variable valence. The optimal concentration ratio of electrolyte components $c(Fe^{3+}):c(Cit^{3-}):c(MoO_4^{2-})$ is 1.0:1.5:0.3 and a change of it to the side of an increase in the content of molybdate ions results in the formation of their dimeric forms in the solution and deceleration of cathode process on the whole.

The kinetics of electrochemical deposition of the Fe–W alloy was studied using the solutions with the constant concentrations of iron(III) and ligand; the concentration of tungstate ions varied in the range of 0.004 to 0.008 mol/dm^3. Let us note that in contrast to the electrolyte containing molybdate ions this solution shows a symbate change in pH with an increase in the concentration of tungstate ions (Table 3). A reason for this distinction in the behavior of oxometallates can be explained by their tendency to the polymerization that is predetermined not only by the concentration and pH values but also by the electron envelop structure. As a result the dimerization of tungstates occurs at lower concentrations in comparison with molybdates. In this case, a probability of the progress of reaction (16) that results in the increase of the pH of solution up to 4.3 is increased

$$2WO_4^{2-}+2H^+=W_2O_7^{2-}+H_2O. \quad (16)$$

As for their character, the voltammograms of tungsten reduction in the Fe^{3+}–WO_4^{2-}–Cit^{3-} system are identical to polarization relationships for Fe^{3+}–Cit^{3-} and Fe^{3+}–MoO_4^{2-}–Cit^{3-} systems. However, at equal initial concentrations of tungstate ions and molybdate ions (0.006 mol/dm^3) the current density is lower in the studied range of potentials in case of joint reduction of iron and tungsten (Fig. 1). The peak expansion and its degeneration into the wave can be indicative of the availability of previous chemical reaction and the complication of process by the adsorption as one can see from Fig. 1, the dependence 3. It should be noted that in the presence of molybdate and tungstate ions we observed the shift of stationary potentials of the steel electrode to the region of more negative values with regard to Fe^{3+}–Cit^3 system, and it is possibly related to the passivation of steel substrate with oxidizing anions. Simultaneously, the peak of potentials is shifted to the region of more positive values. It means that the joint reduction of iron with oxo-metallates proceeds with the depolarization.

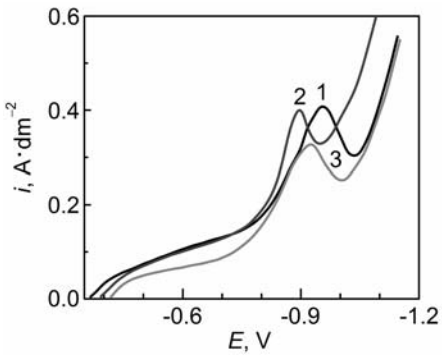

Fig. 1. Polarization dependences for the steel electrode in the electrolytes of composition (mol/dm^3): 1 – 0.03 Cit^{3-}, 0.02 Fe^{3+}; 2 – 0.03 Cit^{3-}, 0.02 Fe^{3+}, 0.006 MoO_4^{2-}; 3 – 0.03 Cit^{3-}, 0.02 Fe^{3+}, 0.006 WO_4^{2-} in 1 M Na_2SO_4 solution as supporting electrolyte; s=2·10^{-2} V/s

Taking into account the tendency of tungstates to the formation of isopolyanions the level of which is defined not only by pH, but also by the concentration of tungstates and the presence of mono-and deprotonated citrate ion(III) clusters $[FeHCit]^+$ ($pK_н$=6.3) and [FeCit] ($pK_н$=11.7) [15] in the studied range we can assume that the two groups of specified particles interact with the formation of hetero-nuclear clusters of a varied composition:

$$[FeCit]+WO_4^{2-}=[FeWO_4Cit]^{2-}; \quad (17)$$

$$[FeHCit]^++WO_4^{2-}=[FeWO_4HCit]^-; \quad (18)$$

$$[FeCit]+W_2O_7^{2-}=[FeW_2O_7Cit]^{2-}; \quad (19)$$

$$[FeHCit]^++W_2O_7^{2-}=[FeW_2O_7HCit]^-. \quad (20)$$

The fact that the maximum peak current density was registered at the minimum concentrations of tungstate in the electrolyte for the studied range also speaks in favor of the assumption on the formation of dimeric forms of tungstates (Table 3). An increase in the content of tungstates predictably results in

Table 3

Kinetic parameters for the system Fe^{3+}–Cit^{3-}–WO_4^{2-} (c, mol/dm^3: Na_2SO_4 1; Fe^{3+} 0.02; Cit^{3-} 0.03; s=2·10^{-2} V/s)

$c(WO_4^{2-})$, mol/dm^3	pH before electrolysis	pH after electrolysis	i_p, A/dm^2	E_p, V	$E_{p/2}$, V	X_s	αz
0.004	3.65	4.1	0.41	–0.95	–0.83	0.45	0.40
0.006	4.00	4.2	0.33	–0.93	–0.81	0.44	0.40
0.008	4.3	4.3	0.29	–0.89	–0.75	0.45	0.34

the formation of their dimeric forms $W_2O_7^{2-}$ and the clusters $[FeW_2O_7HCit]^-$ and in this case the concentration of $[FeWO_4HCit]^-$ clusters out of which tungsten is co-deposited into the alloy according to [11] is decreased and consequently we observe a considerable decrease in the rate of process (Table 3).

The values of αz product calculated using formula (7) for the irreversible phase give grounds to assume that the limiting stage of electrode reaction is the transfer of two electrons, which is indicative of the step reduction of tungsten (VI). An increase in the values of criterion i_p/c at low concentrations of tungstate ions and an increase in the peak current density with an increase in the potential scanning rate are both indicative of the reagent adsorption as in the case of molybdate ions. In addition to the negative values of the concentration criterion, a deviation of $i_p - \sqrt{s}$ relation from the linear one with an increase in the concentration of tungstate ions in the solution is also indicative of the availability of chemical stage. Besides, a negative value of the concentration criterion and the inversion of the values of an apparent order of the reaction in terms of tungsten ions (Table 4) are indicative of the availability of ultimate concentration of tungstate ions, whose increase results in an increase of a probability of the progress of previous chemical reaction. Taking into consideration availability of the combined reaction of hydrogen release that results in the alkalization of near-electrode layer and the fact that a discharge of the clusters with a lower number of ligands occurs easier, it will be logical to assume that such a reaction for specified conditions will represent the formation of hetero-nuclear mono-tungstate-citrate cluster:

$$[FeW_2O_7HCit]^- + 2OH^- = [FeWO_4HCit]^- + (WO_4^{2-}) + H_2O. \quad (21)$$

Table 4

Concentration criterion X_c and apparent order of the reaction in terms of WO_4^{2-} for system Fe^{3+}–Cit^{3-}–WO_4^{2-} (in 1 M Na_2SO_4 solution as supporting electrolyte, $s=2\cdot10^{-2}$ V/s)

$c(Fe^{3+})$, mol/dm^3	$c(Cit^{3-})$, mol/dm^3	$c(WO_4^{2-})$, mol/dm^3	X_c	p_i
0.02	0.03	≤ 0.006	–0.5	0
		≥ 0.006		0.5

At the same time, the relationship E_p–lgs nonlinearity and the tendency of the dependence $E_p - \sqrt{s}$ to the linearization with an increase in the

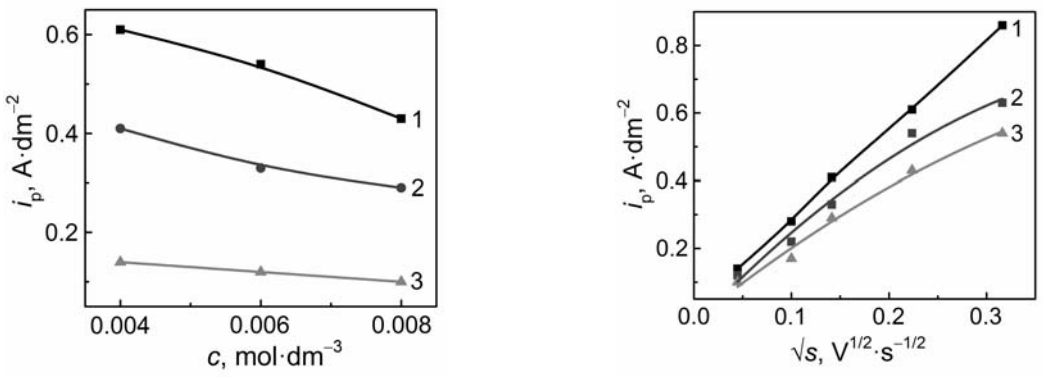

a **b**

Fig. 2. The peak current density vs. the concentration of WO_4^{2-} (a) at s, V/s: 1 – $5\cdot10^{-2}$; 2 – $2\cdot10^{-2}$; 3 – $2\cdot10^{-3}$; and vs. the potential scan rate (b) at $c(WO_4^{2-})$, mol/dm^3: 1 – 0.004; 2 – 0.006; 3 – 0.008

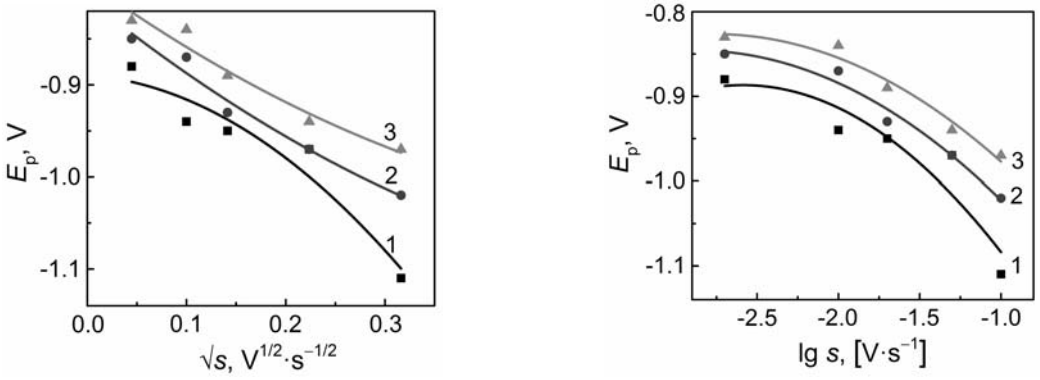

a **b**

Fig. 3. The peak potential vs. potential scan rate in the solution (mol/dm^3): 1 Na_2SO_4, 0.02 Fe^{3+}, 0.03 Cit^{3-}; the concentration of WO_4^{2-} is varied as: 1 – 0.004; 2 – 0.006; 3 – 0.008

concentration of tungstate ions are indicative of the availability of subsequent chemical reaction and the formation of surface phase oxides, which proves a multistage mechanism of the tungstate ions reduction. Since the hydrogen recombination reaction is limiting for iron subgroup metals at high current densities, it is evident that the subsequent chemical reaction will be that of the interaction of tungsten oxides of a variable valence on the electrode surface with the hydrogen ad-atoms with subsequent tungsten to metal reduction.

Based on the analysis of experimental data and taking into consideration the obtained values of kinetic parameters of the electrode reaction we can assume that co-deposition of tungsten into the alloy alongside with the reaction (21) corresponds to the following mechanism:

$$[FeHCitWO_4]^-_L \leftrightarrow [FeHCitWO_4]^-_S; \quad (22)$$

$$[FeHCitWO_4]^-_S + 3\bar{e} + 3H^+ \rightarrow \rightarrow [FeWO_2Cit]^-_S + 2H_2O; \quad (23)$$

$$[FeWO_2Cit]^-_S \leftrightarrow [FeWO_2]^{2+}_S + Cit^{3-}_L; \quad (24)$$

$$[FeWO_2]^{2+}_S + 4H^+ + 6\bar{e} \leftrightarrow Fe|W + 2H_2O, \quad (25)$$

where the indices «L» and «S» are referred to the particles in the solution volume and on the electrode surface, accordingly.

Thereat, a portion of tungsten oxide (IV) can be reduced by hydrogen ad-atoms in the subsequent chemical reaction:

$$[Fe|WO_2]_S + 4H_{ad} \leftrightarrow Fe|W + 2H_2O. \quad (26)$$

Thus, the reduction of tungstate ions and molybdate ions occurs at least in two steps, and the reduction of alloying components will occur on competitive basis for deposition of the ternary alloy Fe–Mo–W.

The studies of the kinetics of cathode deposition of ternary alloy were carried out at the background of 1 M Na_2SO_4 and the constant content of Fe^{3+}, Cit^{3-}, MoO_4^{2-} ions, varying the concentration of tungstate ions (see Table 1). It should be noted that the addition of tungstates into the base solution as in the case of Fe^{3+}–Cit^{3-}–WO_4^{2-} results in a considerable increase in the pH of electrolyte (Table 5), moreover a probability of the formation of mono-forms of the oxo-metallates is rather high, and these are included into the composition of electrode-active clusters.

Polarization relationships for the co-reduction of iron with molybdenum and tungsten show the peaks, whose current density is lower in comparison with those obtained for binary alloys Fe–Mo and Fe–W (Fig. 4) and at the potential scanning rates of $1 \cdot 10^{-1}$ V/s and $2 \cdot 10^{-3}$ V/s the peak is degenerated into the wave. The slope of polarization relationships in the potential range of −0.40 to −0.90 V becomes smoother and this can be indicative of an increase in kinetic and adsorption complications and at the potentials of −0.90 to −1.00 V the process corresponds to the progress of coupled reactions of the reduction of molybdenum, tungsten and hydrogen.

Table 5

The influence of tungstate ions concentration on the pH of the electrolyte

$c(Fe^{3+})$, mol/dm^3	$c(Cit^{3-})$, mol/dm^3	$c(MoO_4^{2-})$, mol/dm^3	$c(WO_4^{2-})$, mol/dm^3	pH
0.02	0.03	0.006	0.004	4.40
			0.006	4.55
			0.008	5.35

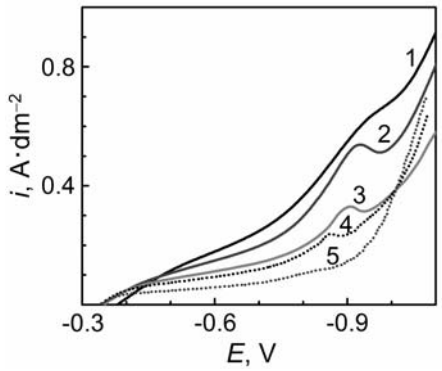

Fig. 4. The polarization dependences for the steel electrode in the solution (mol/dm^3): 0.02 Fe^{3+}, 0.03 Cit^{3-}, 0.006 MoO_4^{2-}, 0.004 WO_4^{2-}. Potential scan rate, s, (V/s): 1 – $1 \cdot 10^{-1}$; 2 – $5 \cdot 10^{-2}$; 3 – $2 \cdot 10^{-2}$; 4 – $1 \cdot 10^{-2}$; 5 – $2 \cdot 10^{-3}$

The calculated values of the Semerano criterion X_s are indicative of the irreversibility of cathode process, and the values of αz calculated using (6) and (7) are perfectly correlated with each other (Table 6) and are indicative of the limiting transfer of two electrons, and it was already noted above that this is peculiar for the step reduction of tungsten by the reactions (14,15).

The behavior of the relationships $i_p - \sqrt{s}$ and $i_p/\sqrt{s} - s$ is also indicative of the irreversibility of cathode process (Fig. 5). A decrease in the values of $i_p/\sqrt{s}$ with an increase in the potential scanning rate is indicative of availability of the chemical phase.

Using a concentration criterion X_c and an apparent order of the reaction p_i of WO_4^{2-}-ions specified an optimal ratio of the concentration of components in the electrolyte $c(Fe^{3+}):c(Cit^{3-}):c(MoO_4^{2-}):c(WO_4^{2-})$ in terms of tungsten ions as 1:1.5:0.3:0.3. Actually, if a probability of the inclusion of oxo-metallates into the composition of hetero-nuclear clusters is used as an optimization parameter,

Table 6

Kinetic parameters for the system Fe^{3+}–Cit^{3-}–MoO_4^{2-}–WO_4^{2-} (c, mol/dm³: Na_2SO_4 1; Fe^{3+} 0.02; Cit^{3-} 0.03; MoO_4^{2-} 0.006)

$c(WO_4^{2-})$, mol/dm³	s, V/s	i_p, A/dm²	E_p, V	$E_{p/2}$, V	X_s	αz	
						(7)	(6)
0.004	$2\cdot10^{-3}$	0.12	–0.84	–0.62	0.45	0.22	0.32
	$1\cdot10^{-2}$	0.24	–0.86	–0.70		0.30	
	$2\cdot10^{-2}$	0.34	–0.91	–0.76		0.32	
	$5\cdot10^{-2}$	0.58	–0.92	–0.80		0.40	
	$1\cdot10^{-1}$	0.68	–0.96	–0.78		0.27	
0.006	$2\cdot10^{-3}$	0.13	–0.85	–0.64	0.39	0.23	0.33
	$1\cdot10^{-2}$	0.27	–0.86	–0.74		0.40	
	$2\cdot10^{-2}$	0.36	–0.92	–0.80		0.40	
	$5\cdot10^{-2}$	0.52	–0.98	–0.80		0.27	
	$1\cdot10^{-1}$	0.64	–1.04	–0.84		0.24	
0.008	$2\cdot10^{-3}$	0.09	–0.82	–0.60	0.50	0.22	0.30
	$1\cdot10^{-2}$	0.21	–0.85	–0.70		0.32	
	$2\cdot10^{-2}$	0.28	–0.87	–0.72		0.32	
	$5\cdot10^{-2}$	0.47	–0.96	–0.80		0.30	
	$1\cdot10^{-1}$	0.61	–0.96	–0.78		0.27	

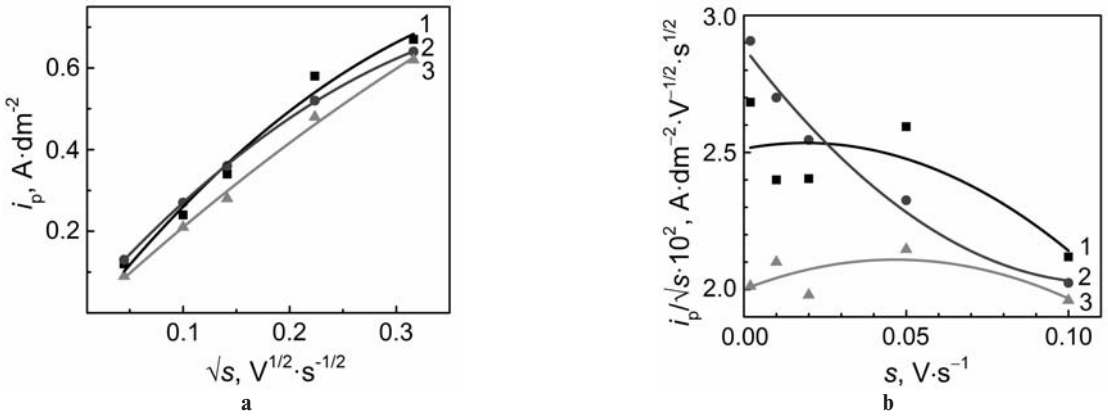

Fig. 5. Peak current density (a) and the characteristic criterion $i_p/\sqrt{s}$ (b) vs. potential scan rate in the electrolyte (mol/dm³): 1 Na_2SO_4, 0.02 Fe^{3+}, 0.03 Cit^{3-}; 0.006 MoO_4^{2-}; $c(WO_4^{2-})$: 1 – 0.004, 2 – 0.006, and 3 – 0.008

the domination of the concentration of molybdates over the tungstates will predictably result in the prevailing of the former in the competition for the place in the hetero-nuclear cluster $[FeHCitMO_4]^-$; and in particular, the negative values of p_i in terms of tungsten ions testify to this (Table 7). Otherwise, an increase in the concentration of tungstates will result in the formation of the clusters that include tungstates and as a consequence a number of particles $[FeHCitWO_4]^-$ will also be increased.

Table 7

Concentration criterion X_c and apparent order of the reaction in terms of WO_4^{2-} for system Fe^{3+}–Cit^{3-}–MoO_4^{2-}– WO_4^{2-} (in 1 M Na_2SO_4 solution as supporting electrolyte, s = $2\cdot10^{-2}$ V/s)

$c(Fe^{3+})$, mol/dm³	$c(Cit^{3-})$, mol/dm³	$c(MoO_4^{2-})$, mol/dm³	$c(WO_4^{2-})$, mol/dm³	X_c	p_i
0.02	0.03	0.006	≤0.006	0.2	–0.33
			≥0.006	–1.0	0.5

Let us note that the concentration criterion X_c is decreased with an increase in the concentration of tungstates from –0.2 to –1.0, which is related to an increase in the probability of realization of the reactions (16), (19) and (20). A value of X_c and the deviation of the relationship i_p/c from the linear character with an increase in the $c(WO_4^{2-})$ concentration is indicative of the availability of previous chemical reaction, and the observed growth of i_p/c (Fig. 6) is indicative of the reagent adsorption. The pH of the near-electrode layer is increased due to the reduction of hydrogen and therefore the assumption about the nature of previous chemical reaction is quite logical (21).

A deviation of the relationship E_p–lgs from the linear shape observed for deposition of the binary alloy and the linearization $E_p - \sqrt{s}$ in case of the Fe–Mo–W deposition are retained (Fig. 7,a and 7,b). The obtained data allow us to make a conclusion that the reduction of tungstates for the deposition of

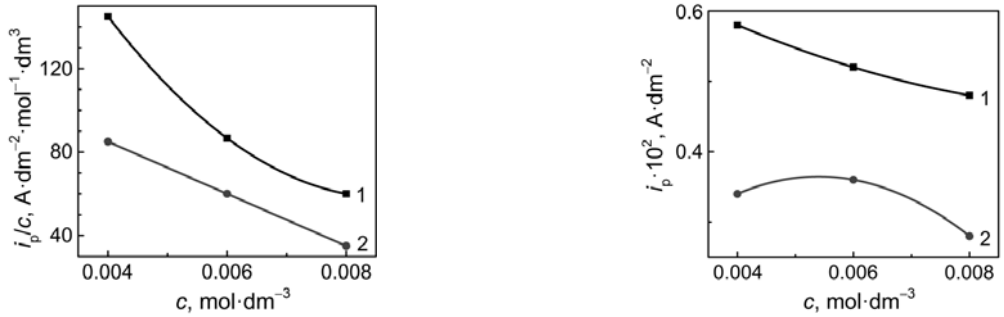

a b

Fig. 6. The characteristic criterion i_p/c (a) and the peak current density (b) vs. the concentration of WO_4^{2-}-ions in the solution (mol/dm^3): 1 Na_2SO_4, 0.02 Fe^{3+}, 0.03 Cit^{3-}; 0.006 MoO_4^{2-}; s (V/s): 1 – $5 \cdot 10^{-2}$; 2 – $2 \cdot 10^{-2}$

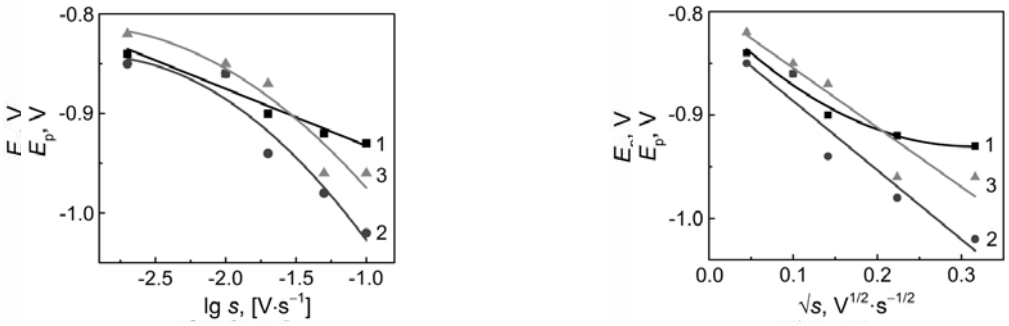

a b

Fig. 7. The peak potential for system Fe^{3+}–Cit^{3-}–MoO_4^{2-}–WO_4^{2-} vs. the potential scan rate in the solution (mol/dm^3): 1 Na_2SO_4; 0.02 Fe^{3+}; 0.03 Cit^{3-}; 0.006 MoO_4^{2-}; c(WO_4^{2-}): 1 – 0.004; 2 – 0.006; 3 – 0.008

coatings by binary Fe–W and ternary Fe–Mo–W alloys proceeds identically and can be described by the system of equations (22–26).

A set of data obtained during the studies of the reduction of individual components and electrocrystallization of the alloys Fe–Mo, Fe–W and Fe–Mo–W allow us to represent a mechanism of the co-deposition of metals into the ternary alloy in the form of generalized diagram (Fig. 8).

The diagram reflects the co-deposition of iron with molybdenum and tungsten into the Fe–Mo (Fe–W, Fe–Mo–W) alloy as the irreversible reduction of intermediates with the limiting discharge step and a preceding chemical step of the ligand release. A suggested diagram takes into account ion hydrolysis reactions, the formation of clusters and polyanions that proceed in the solution with the participation of Fe(III), citrate and oxoanions MoO_4^{2-} (WO_4^{2-}) (Fig. 8, the routes A1, A2 and A3), the iron electrodeposition (B1), coupled reactions of the reduction of molybdenum and tungsten with iron (B2 and B3), the parallel hydrogen release reaction, and also chemical reduction of the intermediate molybdenum and tungsten oxides by hydrogen ad-atoms and a possible coating hydrogenation. The suggested mechanism served as a basis for the development of electrolytes composition to deposit Fe–W and Fe–Mo–W alloys (Table 8).

Table 8

The composition of electrolytes for deposition of Fe–W and Fe–Mo–W coatings

Components	Concentration, mol/dm^3 for deposits	
	Fe–W	Fe–Mo–W
Na_2SO_4	0.10–0.15	0.10–0.15
$Fe_2(SO_4)_3 \cdot 9H_2O$	0.75–0.10	0.75–0.10
$Na_3C_6H_5O_7 \cdot 2H_2O$	0.3	0.3
$Na_2MoO_4 \cdot 2H_2O$	–	0.06–0.08
$Na_2WO_4 \cdot 2H_2O$	0.04–0.06	0.04–0.06
H_3BO_3	0.15–0.20	0.15–0.20

The data of X-ray spectroscopy of the coatings obtained from the electrolytes of a composition corresponding to theoretical relationships at identical electrolysis conditions show a considerable difference in the morphology of binary and ternary alloys (Fig. 9). Binary alloys are characterized by availability of the branched surface with the spheroid structures of a different size and substantial porosity conditioned by an intensive hydrogen release. Fe–Mo–W coatings differ by more uniform and amorphous surface structure that contains grain agglomerates with some pores (Fig. 9,b).

The diffraction pattern of the Fe–W coating (Fig. 10, a) shows two systems of diffraction lines that correspond to the phases with volume-centered cubic crystal lattice (CCL); one of them is related

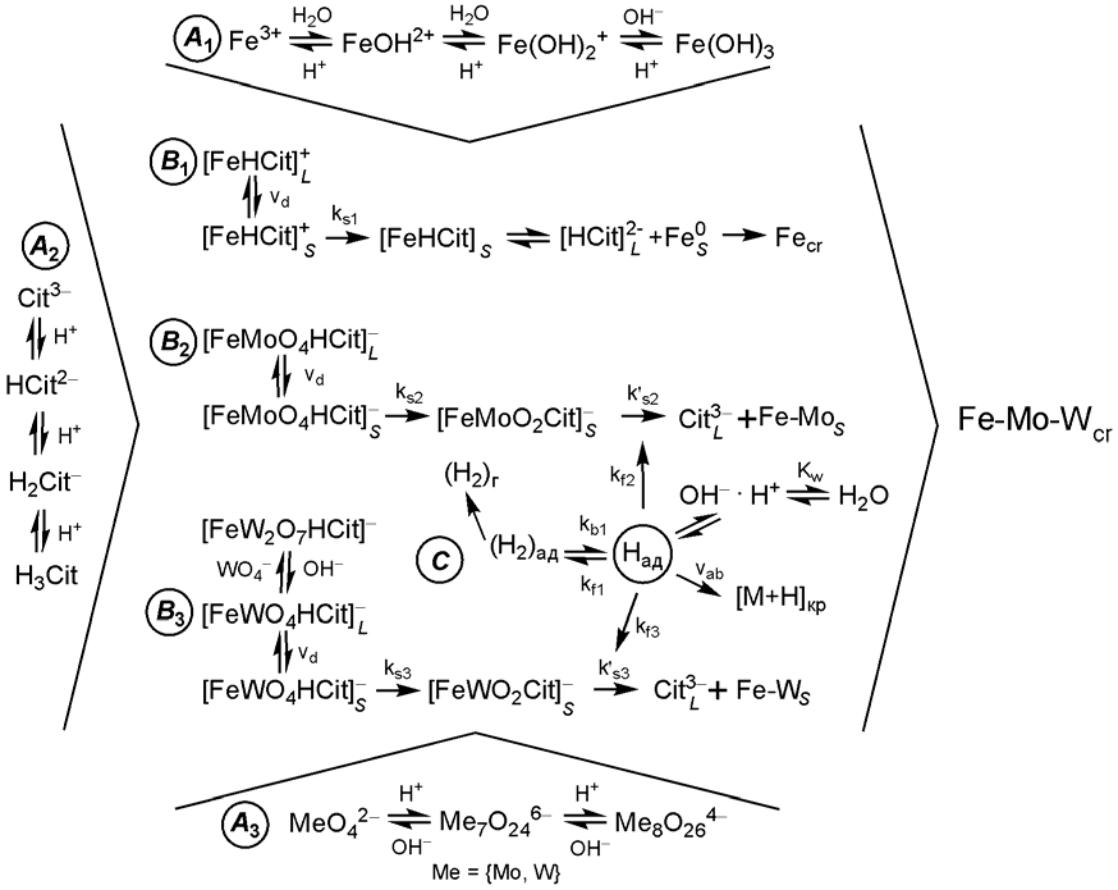

Fig. 8. Fe–Mo–W alloy deposition diagram

to α-Fe (substrate) and another with the lattice period of 2.91 Å corresponds to the solid solution of tungsten in iron. The concentration of tungsten in the solid solution defined using the Vegard rule is equal to 13 at.% and this correlates with the data of X-ray fluorescent spectroscopy and energy dispersive X-ray spectroscopy.

In contrast to the Fe–W alloy the Fe–Mo–W coating is X-ray amorphous and it is characterized by the availability (alongside with the diffraction lines of α-Fe) of a broad halo at low angles (Fig. 10,b) which reflects the amorphous structure of the coating with the ternary alloy.

Conclusions

Experimental investigation data show that for the deposition of Fe–W alloy the cathode process proceeds with the participation of the clusters $[FeHCitWO_4]^-$ and the reduction of tungstate ions has a multistep character through the formation of tungsten oxides of a variable valence.

An optimal ratio of the concentration of components in the electrolyte for deposition of the Fe–W alloy has been defined as $c(Fe^{3+}):c(Cit^{3-}):c(WO_4^{2-})=1:1.5:0.3$. A disturbance of this ratio to the side of an increase in the concentration of tungstate ions results in the formation of dimeric forms $W_2O_7^{2-}$ and $[FeW_2O_7HCit]^-$ clusters and the concentration of electrode-active particles $[FeWO_4HCit]^-$ is reduced and consequently the cathode process is retarded on the whole.

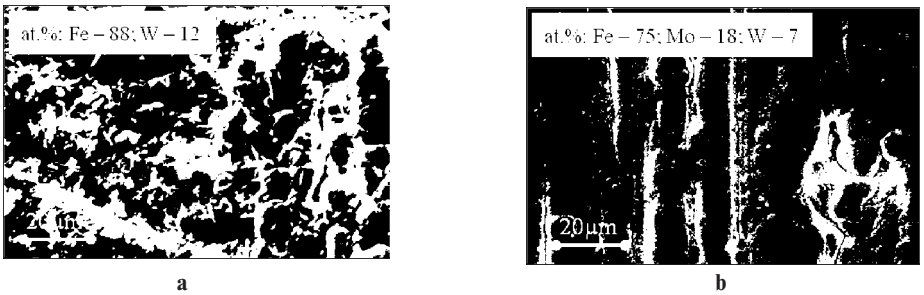

a **b**

Fig. 9. Surface morphology of the Fe–W (a) and Fe–Mo–W (b) coatings formed in the pulse mode (i=5 A/dm²; t_{on}/t_{off}=5/20 ms) on the low-carbon steel substrate

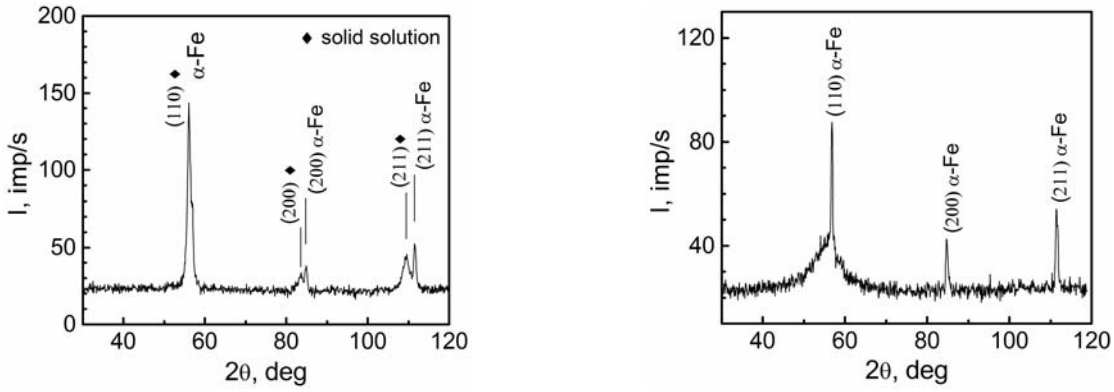

a b

Fig. 10. Diffraction patterns of the Fe–W (a) and Fe–Mo–W (b) coatings formed on the mild steel

It has been established that the reduction of molybdate ions and tungstate ions for the deposition into the Fe–Mo–W alloy occurs on competitive basis and an optimal ratio of the components in the electrolyte is defined as $c(Fe^{3+}):c(Cit^{3-}):c(MoO_4^{2-}):c(WO_4^{2-})$ as 1:1.5:0.3:0.3.

The results obtained for the integrated analysis of experimental data enable the interpretation of the deposition mechanism of Fe–W and Fe–Mo–W alloys as a set of coupled reactions of the reduction of the intermediates with the limiting discharge stage and a previous chemical stage of the ligand release.

The Fe–W coatings deposited out of the electrolyte that were developed taking into account specific features of the mechanism of electrochemical process represent the solid solution of tungsten in iron; and the ternary alloy Fe–Mo–W is X-ray amorphous.

REFERENCES

1. *Synthesis*, Structure and Properties of Nickel-Iron-Tungsten Alloy Electrodeposits – part I: Effect of Synthesis Parameters on Chemical Composition, Microstructure and Morphology / N. Ćirović, P. Spasojević, L. Ribić-Zelenović, P. Mašković, M. Spasojević // Science of Sintering. – 2015. – Vol.47. – P.347-365.

2. *Iron* binary and ternary coatings with molybdenum and tungsten / G. Yar-Mukhamedova, M. Ved', N. Sakhnenko, A. Karakurkchi, I. Yermolenko // Appl. Surf. Sci. – 2016. – Vol.383. – P.346-352.

3. *Gomez E., Pellicer E., Vallés E.* Influence of the bath composition and the pH on the induced cobalt/molybdenum electrodeposition // J. Electroanal. Chem. – 2003. – Vol.556. – P.137-145.

4. *Podlaha E.J., Landolt D.* Induced Codeposition: III. Molybdenum Alloys with Nickel, Cobalt, and Iron // J. Electrochem. Soc. – 1997. – Vol.144. – № 5. – P.1672-1680.

5. *Electroplating* of Amorphous Thin Films of Tungsten/ Nickel Alloys / O. Younes, L. Zhu, Y. Rosenberg, Y. Shacham-Diamond, and E. Gileadi // Langmuir. – 2001. – Vol.17. – № 26. – P.8270-8275.

6. *The anomalous* codeposition of tungsten in the presence of nickel / O. Younes-Metzler, L. Zhu, E. Gileadi // Electrochim. Acta. – 2003. – Vol.48. – P.2551-2562.

7. *Anomalous* Electrodeposition of Co-W Coatings from a Citrate Electrolyte Due to the Formation of Multinuclear Heterometallic Complexes in the Solution / S.S. Belevskii, S.P. Yushchenko, A.I. Dikusar // Surf. Eng. Appl. Electrochem. – 2012. – Vol.48, – № 1. – P.97-98.

8. *Role* of Complexation in Forming Composition of Co–W Coatings Electrodeposited from Gluconate Electrolyte / A.I. Shulman, S.S. Belevskii, S.P. Yushchenko, A.I. Dikusar // Surf. Eng. Appl. Elect. – 2014. – Vol.50. – № 1. – P.9-17.

9. *Elektroosazhdenie* i svoistva splava zhelezo-vol"fram [Electrodeposition and properties of the iron-tungsten alloy] / Zh.I. Bobanova, D.Z. Grabko, Z. Danitse, Ya. Mirgorodskaya, A.I. Dikusar // Elektronnaya obrabotka materialov. – 2007. – Vol.4. – P.12-21.

10. *Danilov F.I., Protsenko V.S., Ubiikon' A.V.* Kinetic Regularities Governing the Reaction of Electrodeposition of Iron from Solutions of Citrate Complexes of Iron(III) // Russ. J. Electrochem. – 2005. – Vol.41. – № 12. – P.1282-1289.

11. *Electrochemical* Deposition of Fe–Mo–W Alloy Coatings from Citrate Electrolyte / A.V. Karakurkchi, M.V. Ved', I.Yu. Ermolenko, and N.D. Sakhnenko // Surface Engineering and Applied Electrochemistry. – 2016. – Vol.52. – № 1. – P.43-49.

12. *Budnikov G.K., Maystrenko V.N., Vyaselev M.R.* Osnovy sovremennogo elektrokhimicheskogo analiza [Fundamentals of contemporary electrochemical analyzis] // Mir Binom LZ Publishers. – Moscow, 2003. – 592 p.

13. *Tochitskiy A., Dmitrieva A.E.* O mekhanizme formirovaniya rentgenoamorfnoi struktury pl'yonok splavov Ni–W [On the mechanism of formation of amorphous structure of Ni–W alloy films] // Metallofiz. noveyshie tehnol. – 2013. – Vol.35. – № 12. – P.1629-1636.

14. *Osobennosti* soosazhdeniya zheleza(III) s molibdenom iz tsitratnyih elektrolitov [Features of the co-precipitation of iron(III) with molybdenum from citrate electrolytes] / I.Yu. Yermolenko, M.V. Ved', N.D. Sakhnenko, A.V. Karakurkchi, T.Yu. Myrnaya // Issues of Chemistry and Chemical Technology. – 2015. – Vol.6(104). – P.47-54.

15. *Electrodeposition* of Iron−Molybdenum−Tungsten Coatings from Citrate Electrolytes / A.V. Karakurkchi, M.V. Ved', N.D. Sakhnenko, and I.Yu. Ermolenko // Russ. J. Appl. Chem. − 2015. − Vol.88. − № 11. − P.1860-1869.

Received 3.04.2017

THE ELECTROCHEMICAL BEHAVIOR OF Fe^{3+}−WO_4^{2-}−Cit^{3-} AND Fe^{3+}−MoO_4^{2-}−WO_4^{2-}−Cit^{3} SYSTEMS

I.Yu. Yermolenko, M.V. Ved', A.V. Karakurkchi, N.D. Sakhnenko, Z.I. Kolupayeva

National Technical University «Kharkiv Polytechnic Institute», Kharkiv, Ukraine

The kinetic parameters of electrochemical behavior of tungsten at the deposition of Fe−W and Fe−Mo−W alloys were determined using linear voltammetry and analyzing polarization relationships. In the presence of citrate ions the cathode process was shown to proceed with the participation of $[FeHCitWO_4]^-$ clusters. An optimal concentration ratio of the components in electrolyte required for the Fe−W alloy deposition was defined as $c(Fe^{3+}):c(Cit^{3-}):c(WO_4^{2-})= =1:1.5:0.3$. The deviation from this ratio by an increase in the concentration of tungstate ions results in the formation of dimer forms $W_2O_7^{2-}$ and $[FeW_2O_7HCit]^-$ clusters; as a result the concentration of electrode active particles $[FeWO_4HCit]^-$ diminishes and the cathode process is inhibited. A peculiar feature of the formation of electrolytic alloy Fe−Mo−W is a competitive reduction of molybdates and tungstates. Based on the analysis of the kinetic parameters and characteristic criteria of electrochemical reactions, we proposed the mechanism for the co-deposition of alloy containing iron with molybdenum and tungsten; this mechanism is a sequence of coupled reactions of irreversible reduction of intermediates with slow charge transfer stage and previous chemical step of the ligands release. The data of X-ray phase analysis show that the binary alloys Fe−W are solid solutions of tungsten in iron and ternary alloys Fe−Mo−W are X-ray amorphous.

Keywords: tungsten; alloys; iron; kinetics; citrate electrolyte; electrodeposition.

REFERENCES

1. Ćirović N., Spasojević P., Ribić-Zelenović L., Mašković P., Spasojević M. Synthesis, structure and properties of nickel-iron-tungsten alloy electrodeposits − part I: Effect of synthesis parameters on chemical composition, microstructure and morphology. *Science of Sintering*, 2015, vol. 47, pp. 347-365. Available at: https://doi.org/10.2298/SOS1503347C.

2. Yar-Mukhamedova G., Ved' M., Sakhnenko N., Karakurkchi A., Yermolenko I. Iron binary and ternary coatings with molybdenum and tungsten. *Applied Surface Science*, 2016, vol. 383, pp. 346-352.

3. Gómez E., Pellicer E., Vallés E. Influence of the bath composition and the pH on the induced cobalt−molybdenum electrodeposition. *Journal of Electroanalytical Chemistry*, 2003, vol. 556, pp. 137-145.

4. Podlaha E.J., Landolt D. Induced codeposition: III. Molybdenum alloys with nickel, cobalt, and iron. *Journal of the Electrochemical Society*, 1997, vol. 144, no. 5, pp. 1672-1680.

5. Younes O., Zhu L., Rosenberg Y., Shacham-Diamand Y., Gileadi E. Electroplating of amorphous thin films of tungsten/nickel alloys. *Langmuir*, 2001, vol. 17, no. 26, pp. 8270-8275. Available at: https://doi.org/10.1021/la010660x.

6. Younes-Metzler O., Zhu L., Gileadi E. The anomalous codeposition of tungsten in the presence of nickel. *Electrochimica Acta*, 2003, vol. 48, pp. 2551-2562.

7. Belevskii S.S., Yushchenko S.P., Dikusar A.I. Anomalous electrodeposition of Co-W coatings from a citrate electrolyte due to the formation of multinuclear heterometallic complexes in the solution. *Surface Engineering and Applied Electrochemistry,* 2012, vol. 48, no. 1, pp. 97-98.

8. Shul'man A.I., Belevskii S.S., Yushchenko S.P., Dikusar A.I. Role of complexation in forming composition of Co−W coatings electrodeposited from gluconate electrolyte. *Surface Engineering and Applied Electrochemistry*, 2014, vol. 50, no. 1, pp. 9-17.

9. Bobanova Z.I., Grabko D.Z., Danitse Z., Mirgorodskaya Ya., Dikusar A.I. Elektroosazhdenie i svoistva splava zhelezo-vol'fram [Electrodeposition and properties of iron-tungsten alloy]. *Elektronnaya Obrabotka Materialov*, 2007, vol. 4, pp. 12-21. (*in Russian*).

10. Danilov F.I., Protsenko V.S., Ubiikon' A.V. Kinetic regularities governing the reaction of electrodeposition of iron from solutions of citrate complexes of iron(III). *Russian Journal of Electrochemistry*, 2005, vol. 41, pp. 1282-1289.

11. Karakurkchi A.V., Ved' M.V., Ermolenko I.Yu., Sakhnenko N.D. Electrochemical deposition of Fe−Mo−W alloy coatings from citrate electrolyte. *Surface Engineering and Applied Electrochemistry*, 2016, vol. 52, no. 1, pp. 43-49.

12. Budnikov G.K., Maystrenko V.N., Vyaselev M.R., *Osnovy sovremennogo elektrokhimicheskogo analiza* [Fundamentals of contemporary electrochemical analysis]. Mir Binom LZ Publishers, Moscow, 2003. 592 p. (*in Russian*).

13. Tochitskiy A., Dmitrieva A.E. O mekhanizme formirovaniya rentgenoamorfnoi struktury pl'yonok splavov Ni−W [On the mechanism of the formation of amorphous structure of Ni-W alloy films]. *Metallofizika i Noveishie Tekhnologii*, 2013, vol. 35, no. 12, pp. 1629-1636. (*in Russian*).

14. Yermolenko I.Yu., Ved' M.V., Sakhnenko N.D., Karakurkchi A.V., Myrnaya T.Yu. Osobennosti soosazhdeniya zheleza(III) s molibdenom iz tsitratnykh elektrolitov [Features of the co-precipitation of iron(III) with molybdenum from citrate electrolytes]. *Voprosy khimii i khimicheskoi tekhnologii*, 2015, vol. 6, pp. 47-54. (*in Russian*).

15. Karakurkchi A.V., Ved' M.V., Sakhnenko N.D., Ermolenko I.Yu. Electrodeposition of iron−molybdenum−tungsten coatings from citrate electrolytes. *Russian Journal of Applied Chemistry*, 2015, vol. 88, no. 11, pp. 1860-1869.